


Dye degradation in water using Nickel/Bismuth catalyst

 <https://doi.org/10.56238/sevened2024.003-071>

Lincoln Fonseca de Souza¹, Diego Guimarães², Rossano Gimenes³ and Flavio Soares Silva⁴

ABSTRACT

The chemical contaminants present in the aquatic environment resources are a major cause of concern for human health and the environment and safety concern. These contaminations have risen into a major threat to the water distribution system. Ultimately, research activities centred on advanced oxidation processes (AOPs) for the destruction of synthetic organic species resistant to conventional methods. AOPs rely on in situ generation of highly reactive radical species, mainly hydroxyl radical ($\cdot\text{HO}$) by using solar, chemical or other forms of energy. The most attractive feature of AOPs is that this highly potent and strongly oxidizing radical allows the destruction of a wide range of organic chemical substrate with no selectivity. Catalysts based on bismuth and nickel shows photocatalytic activity under the action of visible light. Catalysts were prepared by hydrolysis followed by thermal treatment (400°C for 3 hours). Characterization techniques such as X-ray diffraction (XRD), the tetragonal and monoclinic phases were confirmed. Scanning Electron Microscopy (SEM) with Energy-Dispersive X-Ray Spectroscopy (EDS) showed micro-flora morphology hierarchically constructed by stacking nanosheets with thicknesses ranging from 140-250 nm. The calculated E_g values reached 2.36 eV. The photocatalytic efficiency was evaluated under white LED light irradiation for 2 hours. The reaction control parameters were 50 mg of catalyst, 12.00 mg L⁻¹ RhB solution and natural pH of the RhB solution (pH = 6.22). The catalyst showed photocatalytic efficiency of 99%. The synthesized materials showed a high capacity for consecutive reuse, proving to be an environmentally friendly, green chemistry, and economically viable approach.

Keywords: Degradation, Dye, Rhodamine B, Ni/Bi Catalyst, Water.

¹ MSc in Chemistry

Institution: Federal University of Itajubá (UNIFEI)

E-mail: lincolnfs87@unifei.edu.br

² Bachelor of Science in Chemistry

Institution: Federal University of Itajubá (UNIFEI)

E-mail: diegoguimaraes@unifei.edu.br

³ Dr. in Chemistry

Institution: Federal University of Itajubá (UNIFEI)

E-mail: rossano@unifei.edu.br

⁴ Dr. in Chemistry

Institution: Federal University of Itajubá (UNIFEI)

E-mail: flaviosoaresilva@unifei.edu.br

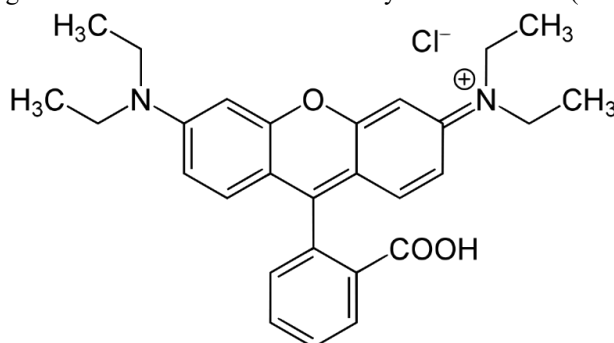
INTRODUCTION

The continuous accelerated growth of the world population, added to the needs of social and economic development, as a consequence, have generated serious environmental problems, which impact society and human life, such as the contamination of drinking water by organic compounds from urban, industrial and agricultural effluents (MENDONÇA, 2014).

Industrial activities such as pesticides, petrochemicals, pharmaceuticals, plastics, pulp and paper, and textile dyes, are responsible for the rapid development of human society, and along with progress come excessive discharges of industrial effluents into water bodies and even groundwater (JIANG et al, 2020).

Many organic pollutants present in water, even in low concentrations, can have adverse effects, such as acute toxicity, endocrine disruption, and can also increase the resistance of harmful pathogens (TORRES, 2019), present high toxicity, mutagenicity, carcinogenicity, thus becoming a major threat to the ecosystem (JIN et al, 2017). Among these pollutants, Rhodamine B stands out (Figure 1), with a molecular formula ($C_{28}H_{31}N_2O_3Cl$), with fluorescent characteristics and a slightly acidic character ($pK_a = 3.8$) (RICHARDSON, 2004).

Figure 1. Molecular structure of the dye Rhodamine B (RhB).



Source: Authored by the authors.

This dye is used in the paper, wood and cellulose derivatives dyeing industries, as well as in textile production segments, such as cotton, silk and leather (SHAIKH, 2020). Even in the face of a wide application in many sectors, RhB has been confirmed as a carcinogen and teratogen, especially for pregnant women and children according to (GUPTA, 2009).

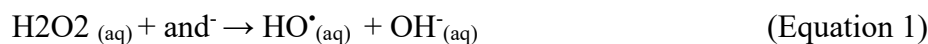
Conventional water treatment techniques, used since decades ago, such as filtration, adsorption, sedimentation, biological and chemical treatments, reverse osmosis, have been exhaustively applied, however, the effectiveness of these techniques is not adequate, causing non-removal and/or complete degradation, and may also produce other harmful by-products, in addition to transferring pollutants to a secondary phase, therefore requiring after-treatment (JIN et al, 2017; THEJASWINI, 2017; SHARMA et al, 2019).



In recent decades, however, the scientific community has been dedicated to the development of new technologies and methods for the treatment of contaminated water, which ensure greater safety and efficiency in removal and/or degradation, or even methodological strategies that are capable of converting harmful substances, and highly dangerous to the ecosystem and human society, into less harmful substances and without secondary pollution.

Different methodologies applied in the treatment of wastewater, endowed with organic contaminants, difficult to remove and/or degrade that have been discussed and developed by the scientific community, without a doubt, the so-called Advanced Oxidative Processes (AOP's) stand out, which consist of techniques with high efficiency in the degradation of different types of non-biodegradable or highly persistent contaminants (MENDONÇA, 2014). These methods are mainly based on the generation of free radicals with high oxidizing power, highlighting the hydroxyl radical ($\cdot\text{OH}$), with oxidation potential $E(\cdot\text{OH} / \text{H}_2\text{O}) = 2.80 \text{ eV}$, in which it is highly capable of oxidizing and mineralizing, in situ and non-selectively, various carbon-containing contaminants up to the generation of CO_2 , H_2O and inorganic ions as end products (SHARMA et al, 2019).

The hydroxyl radical ($\text{HO}\cdot$), it is usually activated through the use of highly oxidizing sources such as hydrogen peroxide (H_2O_2) (Equation 1), ozone (O_3) and also by the use of ultrasound and ultraviolet (UV) light irradiation.



As mentioned above, one of the variants of POA's, the so-called heterogeneous photocatalysis (FH), has attracted a lot of attention in recent decades, due to its green character, being economically viable, compared to other variables such as ozone-containing systems and having good process repetitiveness (NAJAFIAN et al, 2019). This method is based on the generation of oxidizing radicals by irradiation of light on a catalyst material, usually a semiconductor (SC).

Semiconductor photocatalysis has been widely used in different application areas such as water decomposition, degradation/removal of organic contaminants, sterilization, air purification (KUDO, 2009; MAMBA, 2016; XUE et al, 2017). Among conventional semiconductors, TiO_2 has been considered the most popular material due to its low toxicity, cost-effectiveness, relatively high activity, and chemical stability. However, semiconductors such as TiO_2 and ZnO have photocatalytic capacity only under the influence of ultraviolet (UV) radiation (LIU et al, 2018), due to the large band energy ($E_g \cong 3.2 \text{ eV}$).

According to KUDO (2009), photocatalysts consisting of p-block elements exhibit photocatalytic activity under visible light, resulting in an improvement in the mobility of photogenerated charge carriers and increasing light absorption in the visible range. Materials



containing Bi^{3+} , especially semiconductors, show high photocatalytic activities under visible light irradiation, due to a narrow *band gap* and due to the hybridized valence band (BV) has an electronic structure composed of O 2p and Bi 6s orbitals, while its conduction band (BC) is formed mostly by Bi 6p orbitals (HUANG et al, 2017b). Nickel oxide (NiO) is a p-type semiconductor (acts as an electron acceptor), having nanometric dimensions with better photocatalytic efficiencies than TiO_2 in the degradation of phenol under light irradiation at 266 nm (SUN et al (2018)).

Therefore, it is extremely significant, as well as challenging, to explore the universality and efficiency of new semiconductor-based photocatalyst systems with appropriate band energies, responsive to visible light, economically viable, with good availability, easy to obtain, environmentally friendly and skillful for applications in the removal of various organic pollutants present in water. The objective of this research was to synthesize and characterize a heterostructured compound of Nickel/Bismuth (Ni/Bi) and to evaluate the photocatalytic and recyclability activity in the removal and degradation of the dye Rhodamine B in water under visible light irradiation.

METHODOLOGY

The catalyst was synthesized by the hydrolysis method adapted from NAVALE et al (2020) followed by calcination and combustion at 400°C (3 hours). Two steps were carried out, the first being the synthesis of bismuth oxyiodide, and the second being thermal decomposition together with the formation of nickel oxide.

Nickel nitrate ($\text{Ni}(\text{NO}_3)_2 \cdot 6\text{H}_2\text{O}$) were used in conjunction with BiOI and transferred to an agate mortar with pistil along with 0.1. x grams of citric acid for mechanical homogenization for 10 minutes. Then, the BiOI was added to the mortar and mechanically homogenized for another 10 minutes and transferred to a muffle. The muffle furnace heating schedule consisted of $25 - 150^\circ\text{C}$ ($5^\circ\text{C}/\text{minute}$) maintained for 5 minutes and $150 - 400^\circ\text{C}$ ($5^\circ\text{C}/\text{minute}$) maintained for 3 hours for calcination of the materials and eventual phase transformations of BiOI and NiO formation.

To identify the phases present in the catalyst, X-ray diffraction tests were performed. The parameters used were: voltage 40 kV and current of 40 mA, (scanning range from 10 to 80°). The morphological evaluation of the sample was performed by scanning electron microscope with an X-ray Energy Dispersive Spectroscopy (EDS) detector.

The analyses were performed in a spectrophotometer in diffuse reflectance mode submitted to an average scanning speed in a spectral region from 190 nm to 1400 nm to obtain the spectra.

The absorption spectra in the ultraviolet-visible region of the solutions containing the dye rhodamine B (RhB) were performed using a spectrophotometer with a resolution of 1.5 nm and a scan in the range of 200 to 800 nm. The measurements were performed in a 1.0 cm quartz cuvette.



The tests to evaluate the photocatalytic activity were carried out in an irradiation chamber made of MDF wood (60 cm x 40 cm x 40 cm) containing two cool white LED reflectors (6500 K), with 4500 lumens of luminous flux, efficiency of 90 lm/w, 50 w from the manufacturer INTRAL[®], positioned at the top of the chamber and with the light beams directed to the center of the system containing the solution in a magnetic stirrer. A volume of 100 mL of RhB solution (12 mg L of RhB solution) was used for each assay.⁻¹), at natural pH of the solution (pH = 6.22), added to 34.8 mg of photocatalyst under magnetic stirring. In order to achieve the adsorption/desorption equilibrium of the dissolved dye on the surface of the photocatalyst, they were left for 30 minutes under agitation in the dark and then light irradiation was started for 120 minutes. The efficiency of analyte removal/degradation was calculated according to equation 2 below:

$$\% \text{ Removal Efficiency} = \left(\frac{C_0 - C}{C_0} \right) \cdot 100 \quad (\text{Equation 2})$$

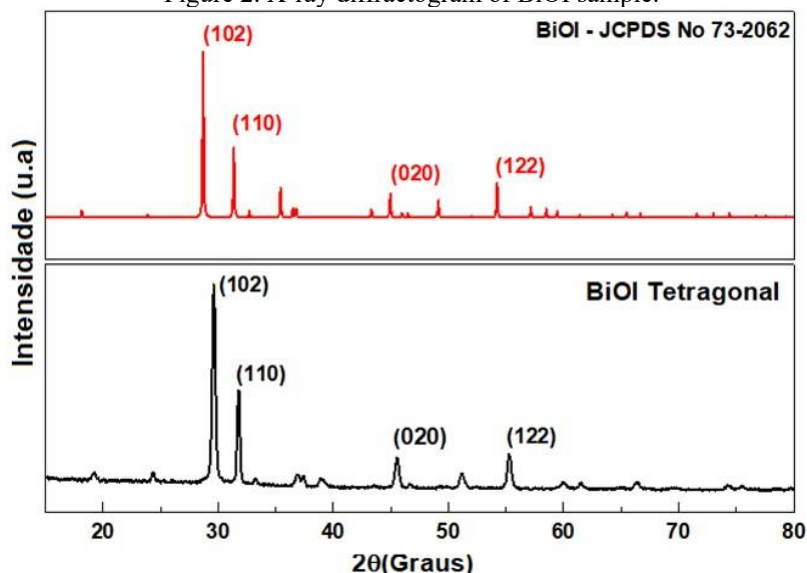
Where C is the concentration at the given time t and C_0 is the initial concentration of the dye to be evaluated. The aliquots were removed at equal intervals, 10 minutes, centrifuged for 2 minutes to remove the precipitate and the supernatant taken to the spectrophotometer for readings.

To evaluate the stability and recyclability, the photocatalyst with the best photocatalytic performance in the degradation of RhB was separated from the solution after centrifugation and collected in a container for subsequent washing with water and ethanol, followed by drying for 4 hours at 60 °C and without further purification used in new cycles of photocatalytic reactions.

RESULTS AND DISCUSSIONS

The synthesized samples were analyzed by X-ray diffraction where the phases and crystallinity of the powders obtained were verified. Figure 2 shows the diffractogram of the BiOI material compared to the JCPDS 73-2062 standard.

Figure 2. X-ray diffractogram of BiOI sample.



Source: Authored by the authors.

The peaks observed in the synthesized sample agree with the standards for BiOI. The most intense peaks are at 29.73° ; 31.80° ; 45.53° ; 55.27° that index with the crystalline planes (102), (110), (020) and (122), respectively and are characterized as a tetragonal crystal lattice. The indexed peaks and planes are in full agreement with those reported in the literature according to HU et al., (2020). The sample showed good crystallinity.

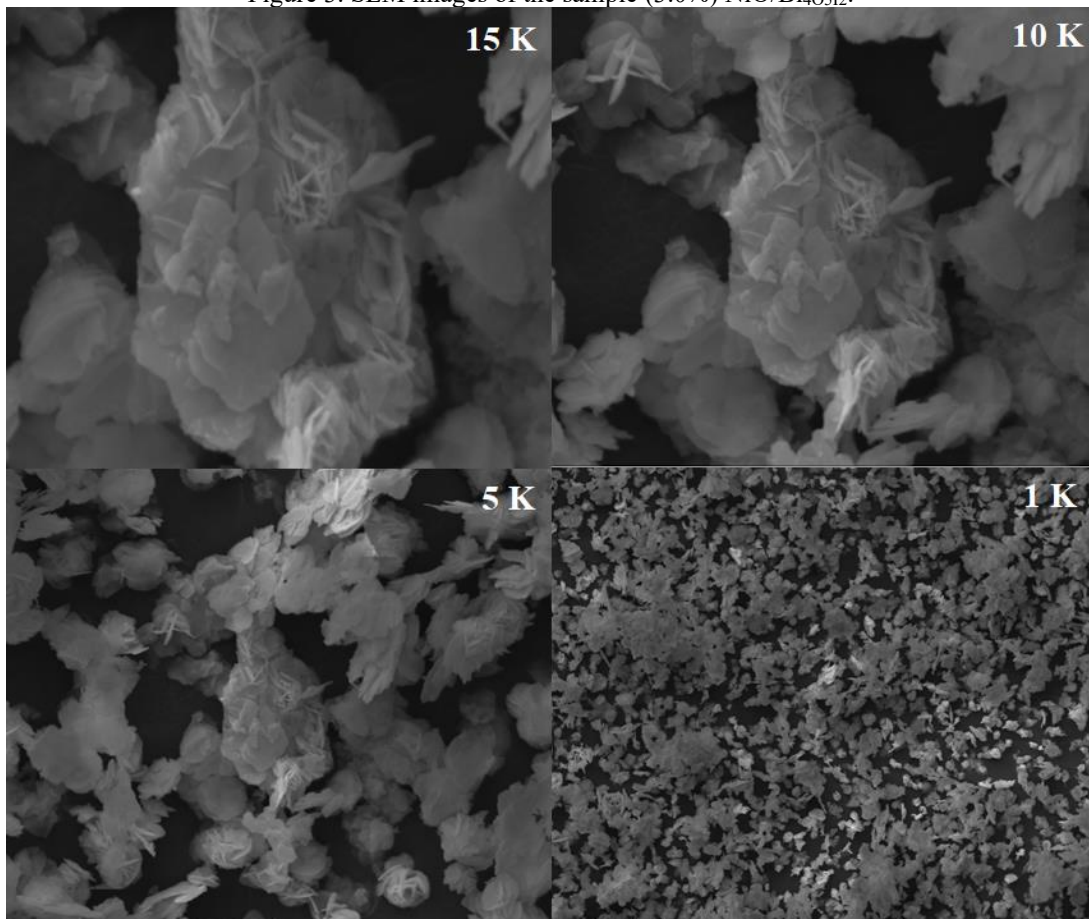
The mean sizes of the crystallites were calculated for the samples obtained using the Scherrer equation (Equation 3):

$$D = \frac{(0,9.\lambda)}{\beta.\cos \theta} \quad (\text{Equation 3})$$

Where D is the average of the crystallites sizes in nanometers, 0.9 is a constant (k) that depends on the shape of the particles (considering a sphere, $k = 0.9$), λ is the wavelength of the electromagnetic radiation, β is the width at half height of the diffraction peak, and θ is the diffraction angle. The calculated values of the mean crystallite sizes ranged from 11-18 nm.

The images obtained through Scanning Electron Microscopy (SEM) for the NiO/Bi₄O₅I₂ sample are shown below in Figure 3. There is a good level of stacking of nanosheets and a noticeable distribution of different sizes. Citric acid was used in the preparation of samples with 1.5 and 3.0 % nickel precursor, and it is expected that the combustion of citric acid will release gases, which in turn helps in the formation of pores in the material.

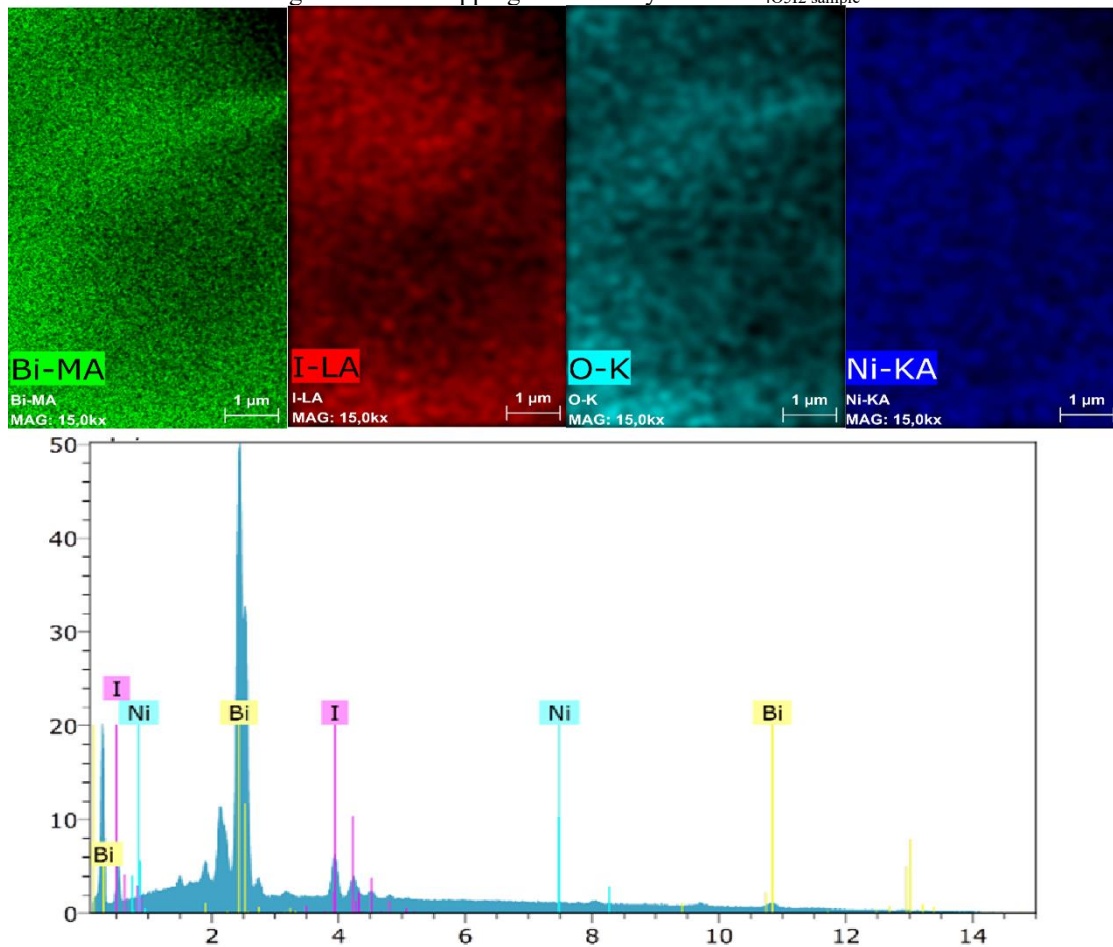
Figure 3. SEM images of the sample (3.0%) NiO/Bi₄O₅I₂.



Source: Authored by the authors.

The EDS of the synthesized samples was also performed and the elemental mapping expresses the absence of other elements, therefore, the sample has no impurities, indicating that the method of choice to obtain the materials was adequate and effective, as shown in Figure 4.

Figure 4. EDS mapping of the catalyst: NiO/Bi₄O₅I₂ sample.



Source: Authored by the authors.

The samples were analyzed by Diffuse Reflectance Spectroscopy (DRS) to verify the photoactive capacity of the materials. Or *band-gap* of the samples was determined by plotting the graph using the Tauc method by using equation 4:

$$(\alpha h\nu)^{1/2} = A(h\nu - E_g) \quad (\text{Equation 4})$$

Where A , h , α and ν represent a constant, Planck's constant, absorption coefficient and frequency of radiation. Therefore, by plotting the graph $(\alpha h\nu)^{1/2}$ versus $h\nu$, the E_g of the material can be estimated by linear fitting by intersecting the axis of the abscissas.

The absorbance spectrum for the BiOI sample shows good radiation absorption in the visible range having an absorption boundary at 657 nm. This result is in agreement with data reported in the literature (QIN et al 2020; HU et al 2020) and, therefore, the sample obtained is active to solar radiation.

The value of the *Band Gap* as expected, had an increase compared to the BiOI sample (1.77 eV), in which the value obtained for NiO/Bi₄O₅I₂ was 2.36 eV, which is in agreement based on the

reports of MA et al (2020). The existence of deviations in the values obtained between the experimental data and the reported data can be attributed to several factors such as: particle size obtained, synthesis methods, precursor reagents and treatment temperatures.

The photocatalytic tests were first conducted under fixed conditions of working parameters such as: solution volume, initial pH (solution itself), target molecule concentration and photocatalyst charge. The adjusted values of the initial work parameters (Table 1) followed trends based on data found in the literature and based on the minimum generation of waste after photocatalytic treatment.

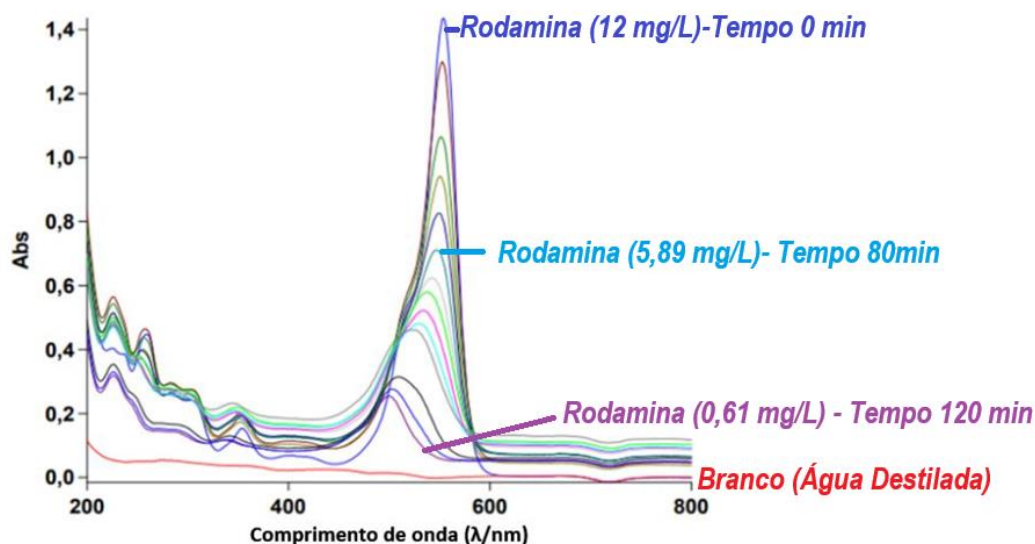
Table 1. Values of photocatalytic parameters.

Volume (mL)	Initial pH	Concentration (mg. L-1)	Photocatalyst Mass (mg)
100	6,22	12,00	34,8

Source: Authored by the authors.

A very relevant piece of information is the photostability of the substance to be studied and, therefore, it is necessary to perform a test with the presence of light and the absence of a photocatalyst. In photolysis, the concentration of RhB decreased by approximately 2.0%, which indicates that the phenomenon responsible for the decrease in its concentration is in fact the presence of the photocatalyst under light irradiation. Figure 5 shows the curves obtained for the photocatalytic assays by comparing the prepared samples.

Figure 5: Absorption spectra of rhodamine B with catalyst and with radiation (CCCR) under different time intervals (0-120 min).

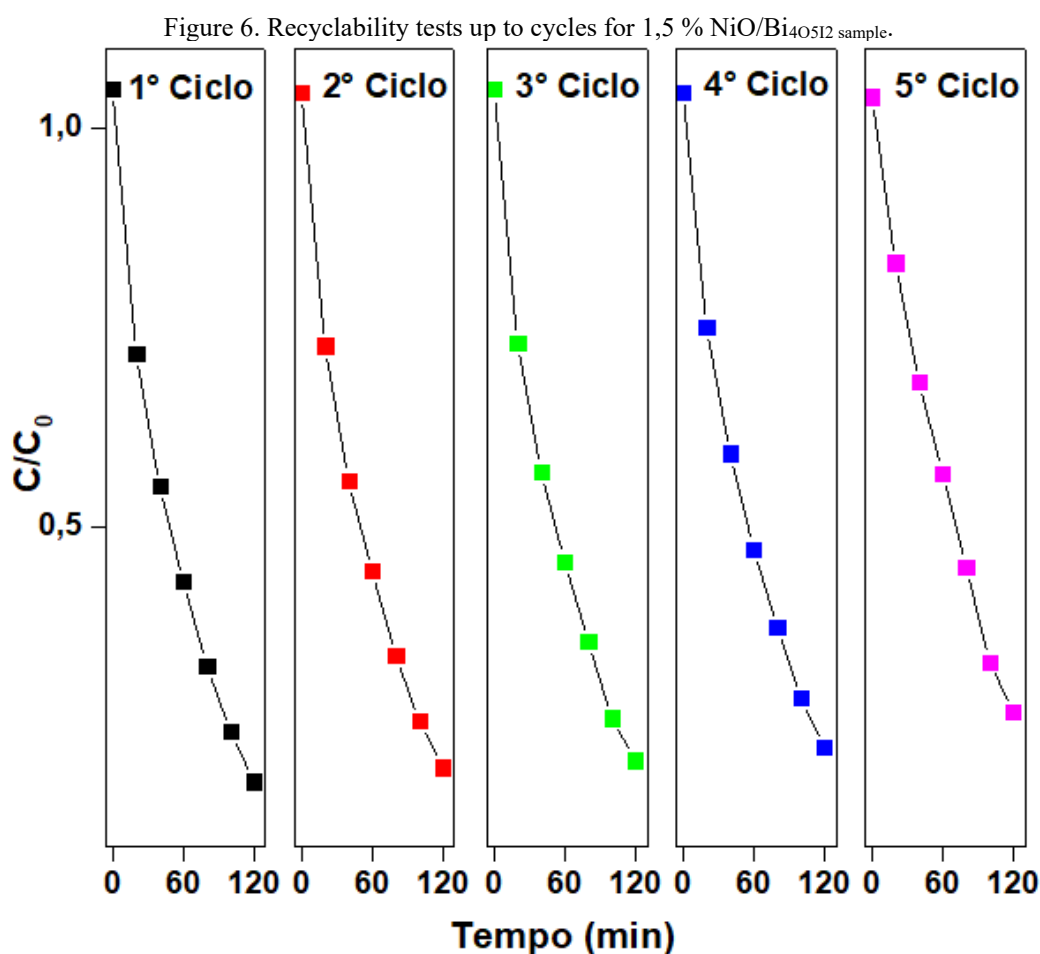


The spectrophotometric calibration curve was plotted (Abs x C) at a wavelength of 550 nm, discarding the points outside the linear range, allowing the construction of a calibration curve with a better correlation coefficient ($R^2 = 1.0000$), showing a working range at concentrations from 0.25 to

12.00 mg L⁻¹. The photocatalytic performance of the control samples showed results with degradation of the dye below 15.89%.

The NiO/Bi_{catalyst 40512} achieved a high degradation efficiency of 99.43% of rhodamine B in water, where it was possible to verify the decreases in the maximum peak intensities at 550 nm referring to the chromophore group of the dye. The samples of catalysts heat treated at 400 °C showed a decrease in the level of particle aggregation, being obtained smaller sizes of crystallites, added to this, the phase transition to bismuth-rich compounds causes a decrease in the recombination rates of the electron/hole pairs, as well as in the adjustment of the BV and BC potentials of the materials, which is reflected in the significant improvement of the photocatalytic efficiency of rhodamine B in water.

In order to verify the stability and recyclability of the photocatalyst material, consecutive cycle tests were performed, as it is an important factor to be considered for practical applications. Figure 6 shows the curves obtained for 5 consecutive cycles for the 1.5 % NiO/Bi sample₄₀₅₁₂ which showed the best photocatalytic performance among the other prepared materials.



Source: Authored by the authors.



From the curves obtained, it is possible to verify a high recyclability in the photocatalytic performance, since until the 5th cycle there were no significant changes in the calculated concentrations. Indirectly, we can affirm that the prepared material also has a high stability, because, otherwise, if it undergoes structural changes during the photocatalytic tests, the material would not present a high level of recyclability.

CONCLUSION

From simple and common precursors it was possible to synthesize materials with unique structural characteristics with photoactive capabilities, where they were applied in a photocatalytic chamber irradiated by artificial light of the white LED type for the study of removal/degradation of the dye Rhodamine B.

The initially synthesized material was heat-treated at 400 °C for 3 hours combined with a combustion reaction in solution with the addition of a nickel precursor salt, where optical and photocatalytic properties were evidenced.

Using techniques such as XRD, SEM-EDS, ERD, the crystalline phases, as well as the morphology of the microflora type and the calculated values for the forbidden band energies (*band gap*) were verified.

The photocatalytic activities were evaluated and the material 1.5% NiO/Bi₄O₅I₂ showed superior performance (99.43% efficiency) for degradation of the dye rhodamine B in water. The evaluation of stability and recyclability showed high stability up to the 5th consecutive cycle, being a favorable point for practical application.

Therefore, based on simplified and low-cost synthetic mechanisms, with a low-consumption energy source (LED), a promising material to be used in the process of heterogeneous photocatalysis irradiated by artificial light was achieved for the degradation of rhodamine B dye in water.

ACKNOWLEDGMENTS

Thanks to FAPEMIG, CAPES and the Multicenter Graduate Program in Chemistry of Minas Gerais (PPGQ-MG).



REFERENCES

1. Gupta, V. K., & Suhas. (2009). Application of low-cost adsorbents for dye removal – A review. *Journal of Environmental Management, 90*(8), 2313 – 2342.
2. Hu, H., et al. (2020). Step-scheme NiO/BiOI heterojunction photocatalyst for rhodamine photodegradation. *Applied Surface Science, 511*, 145499.
3. Huang, H., et al. (2017). Rational design on 3D hierarchical bismuth oxyiodides via in situ self-template phase transformation and phase-junction construction for optimizing photocatalysis against diverse contaminants. *Applied Catalysis B: Environmental, 203*, 879-888.
4. Jiang, E., et al. (2018). Visible-light driven Ag/Bi₃O₄Cl nanocomposite photocatalyst with enhanced photocatalytic activity for degradation of tetracycline. *RSC Advances, 8*(65), 37200-37207.
5. Jin, X., et al. (2017). Bismuth-rich bismuth oxyhalides for environmental and energy photocatalysis. *Coordination Chemistry Reviews, 349*, 84 – 101.
6. Kudo, A., & Miseki, Y. (2009). Heterogeneous photocatalyst materials for water splitting. *Chemical Society Reviews, 38*(1), 253-278.
7. Liu, H., et al. (2018). One-pot hydrothermal synthesis of SnO₂/BiOBr heterojunction photocatalysts for the efficient degradation of organic pollutants under visible light. *ACS Applied Materials & Interfaces, 10*(10), 28686-28694.
8. Ma, Y., et al. (2020). Construction of polythiophene/Bi₄O₅I₂ nanocomposite to promote photocatalytic degradation of a bisphenol A. *Journal of Alloy and Compounds, 82*, 153773.
9. Mamba, G., & Mishra, A. K. (2016). Graphitic carbon nitride (g-C₃N₄) nanocomposite: A new and exciting generation of visible light driven photocatalyst for environmental pollution remediation. *Applied Catalysis B: Environmental, 198*, 347-377.
10. Mendonça, V. R. de. (2014). Síntese e propriedades fotocatalíticas de heteroestruturas TiO₂/SnO₂. Tese de Doutorado, Universidade Federal de São Carlos.
11. Najafian, H., et al. (2019). Enhanced photocatalytic activity of a novel NiO/Bi₂O₃/Bi₃ClO₄ nanocomposite for the degradation of azo dye pollutants under visible light irradiation. *Separation and Purification Technology, 209*, 6-17.
12. Navale, S. T., et al. (2020). Room temperature solid-state synthesis of mesoporous BiOI nanoflakes for the application of chemiresistive gas sensors. *Materials Chemistry and Physics, 241*, 122293.
13. Qin, H., et al. (2020). Ultrasonic-assisted fabrication of a direct Z-scheme BiOI/Bi₂O₄ heterojunction with superior visible light-responsive photocatalytic performance. *Journal of Alloys and Compounds, 821*, 153417.
14. Richardson, S. D., Wilson, C. S., & Rusch, K. A. (2004). Use of rhodamine water tracer in the marshland upwelling system. *Ground Water, 42*, 678-688.
15. Shaikh, W. A., Chakraborty, S., & Islam, R. U. (2020). Photocatalytic degradation of rhodamine B under UV irradiation using Shorea robusta leaf extract mediated bio synthesized silver nanoparticles. *International Journal of Environmental Science and Technology, 17*, 2059-2072.



16. Sharma, K., et al. (2019). Recent advances in enhanced photocatalytic activity of bismuth oxyhalides for efficient photocatalysis of organic pollutants in water: A review. *Journal of Industrial and Engineering Chemistry, 78*, 1-20.
17. Sun, X., et al. (2018). Heterostructure nano-NiO/BiOCl composite with advanced adsorption and photocatalytic performance for organic dye. *Journal of Alloys and Compounds, 736*, 22-28.
18. Thejaswini, T. V. L., Prabhakaran, D., & Akhila Maheswari, M. (2017). Ultrasound assisted synthesis of nano-rod embedded petal designed α -Bi₂O₃-ZnO nanoparticles and their ultra-responsive visible light induced photocatalytic properties. *Journal of Photochemistry and Photobiology A: Chemistry, 335*, 217-229.
19. Torres, C. F. (2019). Síntese, modificação, caracterização e mecanismos de formação de semicondutores fotoativos a base de bismuto. Tese de Doutorado, Universidade de São Paulo.
20. Xue, C., et al. (2017). Anchoring tailored low-index faceted BiOBr nanoplates onto TiO₂ nanorods to enhance the stability and visible-light-driven catalytic activity. *ACS Applied Materials & Interfaces, 9*(9), 16091-16102.